ELSEVIER

PII: S0032-3861(98)00255-9

Polymer Vol. 39 No. 26, pp. 7099–7112, 1998

0032-3861/98/$ - see front matter

Modelling particle size distributions and secondary particle formation in emulsion polymerisation

Emma M. Coen[a], Robert G. Gilbert[a,*], Bradley R. Morrison,[b] Hartmann Leube[b] and Sarah Peach[b]

[a]*School of Chemistry, University of Sydney, Sydney, NSW 2006, Australia*
[b]*BASF ZKD, BASF ZK-Kunststofflaboratorium B 1, Polymer Research Division, BASF Ludwigshafen D-67056, Germany*
(Accepted 19 March 1998)

An extensive model is given for the particle size distribution (PSD), particle number, particle size and amount of secondary nucleation in emulsion polymerisations. This incorporates what are thought to be all of the complex competing processes: aqueous phase kinetics for all radical species arising from both initiator and from exit (desorption), radical balance inside the particles, particle formation by both micellar and homogeneous nucleation mechanisms, and coagulation (the rate of which is obtained using the Healy–Hogg extension of DLVO theory). The predictions of the model are compared to extensive experimental results on rates, time evolution of the particle size distribution, and relative amounts of secondary nucleation, for styrene initiated by persulfate with sodium dodecyl sulfate and with sodium dihexyl sulfosuccinate as surfactants. For this system values of almost all of the many parameters needed for the model are available from independent measurements, and thus no significant parameter adjustment is plausible. Accord with experiment is imperfect but quite acceptable, supporting the validity of the various mechanisms in the model. Effects such as the experimental variation of particle number with ionic strength, as well as calculated coagulation rate coefficients as functions of particle size, suggest that coagulation of precursor (i.e., newly-formed) particles is a significant effect, even above the cmc. The modelling also suggests why secondary nucleation occurs readily in systems stabilised with polymeric surfactant.

(Keywords: emulsion polymerization; free radical; styrene)

Glossary of Symbols

A	Hamaker constant
a_s	minimum area occupied by single surfactant molecule on particle surface
A_{tot}	total surface area of particles
A_s	actual area taken up by one surfactant molecule when adsorbed onto a surface
b_s	Langmuir adsorption isotherm parameter
$B(V,V')$	rate coefficient for coagulation between two particles of volume V and V'
cmc	critical micelle concentration
C_p	monomer concentration within latex particles
C_p^{∞}	upper limit of monomer concentration within the latex particles, for large particles
C_p^{sat}	monomer concentration in the latex particles in the presence of monomer droplets
C_w	monomer concentration in the water phase
C_w^{sat}	monomer concentration in the water phase, in the presence of monomer droplets
d_M	density of monomer
d_p	density of polymer
D_w	diffusion coefficient for monomer in water
[E]	water-phase concentration of desorbed radicals, formed by transfer to monomer
[Elect]	concentration of added electrolyte
e	charge on an electron
[I]	initiator concentration
$[IM_i]$	water-phase concentration of oligomers of degree of polymerisation i, formed from chemical initiator
I_s	ionic strength
j_{crit}	critical degree of polymerisation for particle formation by homogeneous nucleation
K	rate of propagational volume growth per particle
k_B	Boltzmann's constant
k_d	rate coefficient for initiator decomposition
k_{dM}	rate coefficient for desorption of monomeric radicals from particles
k_e^i	rate coefficient for entry of i-meric radical formed by initiator decomposition into pre-existing particles
k_{eE}	rate coefficient for re-entry of desorbed radicals
$k_{e,\,micelle}^i$	entry rate coefficient for micellar capture of oligomeric radicals (i-mers)
k_p^i	propagation rate coefficient of i-meric radical in a particle
k_p	propagation rate coefficient (value of k_p^i for $i \gtrsim 4$)
$k_{p,w}$	water-phase propagation rate coefficient
$k_{p,w}^i$	water-phase propagation rate coefficient for oligomeric radicals of degree of polymerisation i
$k_{t,w}^{i,j}$	water-phase termination rate coefficient between radicals of degree of polymerisation i and j
k_{tr}	rate coefficient for transfer to monomer
[micelle]	concentration of micelles per unit volume of the water phase
M_0	molecular mass of monomer
m_w	mass of monomer dissolved in the water phase
m_M^0	initial mass of monomer in per total volume in the reactor vessel
m_s	mass of monomer required to swell the latex particles
m_p	mass of polymer per total volume in the reactor vessel
m_p^0	mass of polymer per total volume in the reactor volume at time zero
N_A	Avogadro's constant
n_{agg}	aggregation number of the surfactant
N_c	total number of particles per unit volume of the continuous phase
$n_V(V)$ or $n(V)$	number distribution of particles whose unswollen volume is between V and $V + dV$
$n_r(r)$ or $n(r)$	number distribution of particle whose unswollen radius is between r and $r + dr$
$n_0(V)$	number of particles of unswollen volume V that contains zero radicals
$n_1^M(V)$	number of particles of a volume V that contains one monomeric radical
$n_1^P(V)$	number of particles of a volume V that contains one polymeric radical

* To whom correspondence should be addressed

p_{ij}	spin ratio
r	unswollen radius of particle
$r_{micelle}$	radius of a micelle
r_F	particle radius whereafter monomer concentration approaches large-particle value
r_s	swollen radius of particle
R	centre-to-centre separation of two particles
$[R_j]$	water-phase concentration of any radical of degree of polymerisation j
[S]	concentration of added surfactant per unit volume of the water phase
$[S]_w$	concentration of surfactant adsorbed onto the surface of the organic phase, per unit volume of the water phase
T	temperature in Kelvin
V	unswollen volume of particle
V_w	volume of the water phase
V_0	volume at which precursor particles are formed by micellar or homogeneous nucleation
W_{ij}	Fuchs stability ratio
x	fractional conversion of monomer to polymer
z	critical degree of polymerisation for entry
δ	Stern layer thickness
ε	permittivity of water
ε_0	permittivity of free space
ε_r	relative permittivity of water
κ	Debye double layer thickness
σ_r	van der Waals radius of monomer
σ	surface charge density
σ_{surf}	surface charge density due to added surfactant
σ_{gen}	surface charge density due to generated surfactant
ρ	total rate coefficient for entry of all radicals into a latex particle
η	viscosity of water
Ψ	surface potential on a latex particle
Φ_A	attractive potential
Φ_R	repulsive potential
Φ	total potential
ζ	zeta potential of particles

INTRODUCTION

While many (but not all) of the mechanisms governing the growth of seeded emulsion polymerisations are relatively well understood[1], the prediction of phenomena arising from particle formation, such as the particle size distribution, is subject to greater uncertainty. A major problem for realistic modelling is the plethora of mechanisms involved: *Figure 1* (to be discussed in detail later) shows what is thought to be a complete picture of those of kinetic significance. It would therefore seem that genuine a priori prediction is impossible, because of the many unknown rate parameters. Indeed, it is common for modelling studies of particle formation in emulsion polymerisations to predict results which are in very good agreement with experiment, simply because parameter values have been chosen to ensure this. However, mechanistic knowledge is accumulating from *seeded* studies, which avoid the complexity of the processes in *Figure 1* involving particle formation. For such systems at least, there is little latitude in the parameters whose values can be adjusted. Modelling for these systems, and comparison with appropriate data, can therefore be used in a proper test of mechanistic assumptions. In these comparisons, it is essential that use be made of as wide a range of data as possible: for example, it has been noted[2] that the time evolution of the particle size distribution (PSD) is a quantity sensitive to events during particle formation, while the amount of new particles formed in the presence of a pre-existing seed (amount of secondary nucleation) is sensitive to the way in which a radical of sufficient degree of polymerisation forms a particle[3,4]. Sensitive data include the

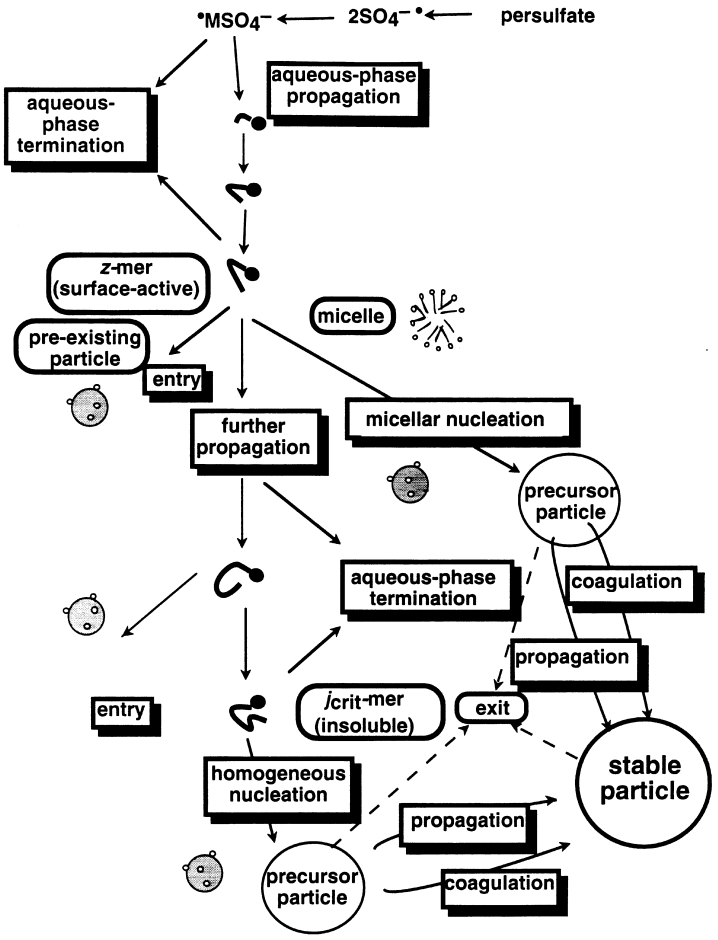

Figure 1 The kinetic events occurring in an emulsion polymerisation

time evolution of the PSD, the particle number and particle size as a function of time, and the overall rate, all during particle formation (of course, these are inter-related). Improvements in instrumentation (such as the advent of analytical ultracentrifugation[5] and of capillary hydrodynamic fraction[6] to measure the PSD) mean that hitherto laborious measurements of some of these quantities are now routine. Comparison between model predictions and data becomes a meaningful test of mechanistic assumptions provided the data cover a sufficient range: e.g., wide variations in surfactant and initiator concentrations, ionic strength, amount of secondary nucleation in a seeded system, etc. models which give adequate accord with such data for systems in which many fundamental parameters are known can be deemed reliable, and can be then used for a priori prediction for new systems. Semi-quantitative predictions of adequate reliability are of particular industrial importance, for example in suggesting conditions whereby secondary particle formation can be minimised.

MODEL

The mechanisms in *Figure 1* (see also the Glossary of Symbols) are as follows[1], and are based on extensive earlier work[6–19]. Initiator decomposes in the water phase (rate coefficient k_d), forming radicals which then react with monomer to form oligomeric radicals in the water phase. These oligomeric radicals (IM_i) can propagate in the water phase (rate coefficient $k^i_{p,w}$), terminate with another radical of degree of polymerisation j (rate coefficient $k^{i,j}_{t,w}$), enter, with second-order rate coefficient $k^i_e(V)$, a pre-existing particle of unswollen volume V if above a critical degree of polymerisation for entry (z), form a particle either by entering micelles if micelles are present in the system (rate coefficient $k^i_{e,micelle}$) or by collapsing if their degree of polymerisation is above a critical degree of polymerisation for homogeneous nucleation (j_{crit}). Radicals within particles can terminate (see below), propagate (rate coefficient k^i_p) or transfer radical activity to monomer (rate coefficient k_{tr}; transfer to chain-transfer agent is trivially incorporated into the description, but is omitted here for notational simplicity).

The monomeric radical formed by transfer may desorb from the particle (rate coefficient k_{dM}). These exited (desorbed) radicals in the water phase are denoted E, and are chemically distinct from water-phase radicals formed directly from initiator. Exited radicals formed by transfer to monomer have a generic formula $M^\bullet$ (in the case of vinyl acetate, for example, the species from transfer is $CH_2CHOCOCH_2^\bullet$, which may subsequently isomerise to a butyrolactonly radical[20–22]). Radicals arising from initiator in the water phase are quite different: for example, if persulfate initiator is used, radicals derived directly from initiator have generic formula $^\bullet M_iSO_4^-$. The most likely fate of desorbed radicals is to re-enter another particle with rate coefficient $k_{eE}(V)$ (it can be easily shown that water-phase propagation and termination with other radicals are very unlikely for desorbed radicals[13,23,24]; moreover, in systems studied here, it is unlikely that exited radicals will enter a micelle and reside sufficiently long therein to create new particles, so that is omitted from the model). Particles grow both by propagation and by coagulation[2,8]; the rate coefficient for coagulation is denoted $B(V,V')$, where V and V' are the unswollen volumes of the pair of coagulating particles[10,11]. For simplicity, termination upon entry of a radical into a particle which already contains a growing chain is assumed to be extremely rapid during particle formation (when particles are small), i.e., the system obeys so-called *zero-one* kinetics (Smith–Ewart cases 1 and 2 combined), so that this rate of termination is simply that of entry[26]. It is convenient to introduce an overall pseudo-first-order entry rate coefficient per particle ρ, which is the total number of entry events per particle per unit time.

The model presented here takes account of the size dependence of various parameters, such as the rate coefficients above and the concentration of monomer in particles. Compartmentalisation is included by distinguishing particles by the number and type of radicals they contain: thus we have the number of particles of unswollen volume V per unit volume of the water phase containing no growing radicals, $n_0(V)$, the corresponding number of particles containing a monomeric radical, $n_1^M(V)$, and those containing a growing chain of degree of polymerisation greater than one, $n_1^P(V)$. It is necessary to distinguish between particles containing monomeric and higher degrees of polymerisation, because only monomeric radicals can exit[27–29].

Radical populations

The rate of change of the water-phase concentration of radicals is given by:

$$\frac{d[IM_1]}{dt} = 2k_d[I] - C_w k^1_{p,w}[IM_1] - [IM_1]\sum_j k^{1,j}_{t,w}[R_j] \quad (1)$$

$$\frac{d[IM_i]}{dt} = C_w(k^{i-1}_{p,w}[IM_{i-1}] - k^i_{p,w}[IM_i]\sum_j k^{i,j}_{t,w}[R_j],$$

$$i = 2, \ldots, z-1 \quad (2)$$

where C_w is the concentration of monomer in the water phase, and R_j denotes any radical of degree of polymerisation j. Equation (1) takes into account the observation that the propagation of an initiator fragment (e.g., $SO_4^{-\bullet}$) with a monomer is so fast as not to be rate-determining[23,30–35]. The concentration of exited radicals in the water phase is given by:

$$\frac{d[E]}{dt} = k_{dM}(V)n_1^M(V) - k_{eE}[E]n(V) - [E]\sum_j k^{i,j}_{t,w}[R_j] \quad (3)$$

where the total particle size distribution and total number concentration of particles are given by:

$$n(V) = n_0(V) + n_1^M(V) + n_1^P(V) \quad (4)$$

$$N_c = N_A\int_0^\infty n(V)dV \quad (5)$$

(N_A being the Avogadro constant). In numerical solution of the various evolution equations, equations (1)–(3) are solved in the steady state, with the resulting non-linear algebraic equations for $[IM_i]$ and [E] solved iteratively.

The evolution equations for the volume distributions are:

$$\frac{\partial N_0(V,t)}{\partial t} = \rho[n_1^P + n_1^M - n_0] + k_{dM}n_1^M - n_0\int_0^\infty B(V,V')[n_0(V') + n_1^P(V')]dV' + \int_0^\infty B(V', V-V')[n_0(V')n_0(V-V') + n_1^P(V')n_1^P(V-V')]dV' \quad (6)$$

$$\frac{\partial n_1^{\mathrm{P}}(V,t)}{\partial t} = \rho_{\mathrm{initiator}}(V)n_0 - \rho(V)n_1^{\mathrm{P}} - k_{\mathrm{tr}}C_{\mathrm{P}}n_1^{\mathrm{P}} - \frac{\partial}{\partial V}Kn_1^{\mathrm{P}} + k_{\mathrm{p}}^1 C_{\mathrm{P}} n_1^{\mathrm{M}} + \delta(V-V_0)\left([\mathrm{IM}_{j_{\mathrm{crit}}-1}]k_{\mathrm{p,w}}^{j_{\mathrm{crit}}-1}C_{\mathrm{w}} + \sum_{i=z}^{j_{\mathrm{crit}}-1}[\mathrm{IM}_i]k_{\mathrm{e,micelle}}^i[\mathrm{micelle}]\right) - n_1^{\mathrm{P}}\int_0^\infty B(V,V')[n_0(V') + n_1^{\mathrm{P}}(V')]\mathrm{d}V' + \int_0^\infty B(V',V-V')[n_0(V')n_1^{\mathrm{P}}(V-V') + n_1^{\mathrm{P}}(V')n_0(V-V')]\mathrm{d}V' \quad (7)$$

$$\frac{\partial n_1^{\mathrm{M}}(V,t)}{\partial t} = -(\rho + k_{\mathrm{p}}^1 C_{\mathrm{p}} + k_{\mathrm{dM}})n_1^{\mathrm{M}} + k_{\mathrm{eE}}[\mathrm{E}]n_0 + k_{\mathrm{tr}}C_{\mathrm{P}}n_1^{\mathrm{P}} \quad (8)$$

$$\rho(V) = \rho_{\mathrm{initiator}}(V) + k_{\mathrm{eE}}(V)[\mathrm{E}];\ \rho_{\mathrm{initiator}} = \sum_{i=z}^{j_{crit}-1} k_{\mathrm{e}}^i(V)[\mathrm{IM}_i] \quad (9)$$

where $C_{\mathrm{P}}(V)$ is the concentration of monomer inside a particle of unswollen volume V, k_{p}^1 is the rate coefficient for propagation, within a particle, of a monomeric radical formed by transfer, [micelle] is the concentration of micelles, V_0 is the volume at which particles are assumed to form after both micellar and homogeneous nucleation, and the propagational growth rate K (the rate of increase in unswollen volume by propagation) is given by:

$$K(V) = \frac{k_{\mathrm{p}}M_0C_{\mathrm{P}}(V)}{N_{\mathrm{A}}d_{\mathrm{p}}} \quad (10)$$

where M_0 is the molecular weight of monomer d_{p} is the density of polymer and k_{p} is the propagation rate coefficient in the particles (this is strictly the long-chain limiting value of k_{p}^i, but propagation becomes independent of chain length for $i >_{\sim} 4$[36]). Equation (7) allows for particle formation by both micellar and homogeneous nucleation mechanisms, through the terms involving $[\mathrm{IM}_i]k_{\mathrm{e,micelle}}^i[\mathrm{micelle}]$ (the rate of entering a micelle to form a precursor particle) and $[\mathrm{IM}_{j_{\mathrm{crit}}-1}]k_{\mathrm{p,w}}^{j_{\mathrm{crit}}-1}C_{\mathrm{w}}$. As set out in equation (7), a surface-active radical may initiate the formation of a particle if it becomes part of a micelle, when the radical centre is in a monomer-rich environment and may thus propagate rapidly. The radical can become part of a micelle either by entering a pre-existing micelle or by a new micelle aggregating around the radical; both events are so rapid as not to be rate determining, since the exchange of surface-active species micelles is extremely fast (on the order of 10^{-6} s), and so the precise mechanism by which a precursor particle forms in the presence of micelles is not kinetically significant. Except extremely close to the critical micelle concentration, the number concentration of micelles, if present, is so much greater than that of particles (whose concentration is in the range) that a surface-active radical is much more like to undergo micellar nucleation than it is to enter a pre-existing particle.

Some of the basic relations, such as equation (7), are most conveniently expressed in terms of the unswollen volume V. Usually, PSDs are given in terms of the unswollen radius r. Introducing for the moment the subscripts r and V to distinguish radius and volume distributions, these two distribution functions are related by[37]:

$$n_V(V) = \frac{N_r(r)}{4\pi r^2} \quad (11)$$

Henceforth, radius and volume distributions will be denoted $n(r)$ and $n(V)$, respectively.

Many of the relations for the various rate parameters, such as $B(V,V')$ and $k_{\mathrm{e}}^i(V)$, are best expressed as functions of the *swollen* radius r_{s}; swollen and unswollen radii are related by:

$$\frac{r_{\mathrm{s}}}{r} = \left(\frac{d_{\mathrm{M}}}{d_{\mathrm{M}} - C_{\mathrm{P}}M_0}\right)^{\frac{1}{3}} \quad (12)$$

where d_{M} is the density of monomer.

Physical parameters

Particle properties. As a result of the competition between the entropy of mixing and surface free energy, the concentration of monomer in the latex particles may be dependent on particle radius. The Morton equation[38] could be used for this dependence, but:

(1) the values of some of the parameters therein, such as the particle/water surface free energy, are uncertain, and
(2) there is increasing evidence that the physical assumptions in this model lead to quantitative (although not qualitative) inaccuracy (e.g.,[39–42]).

For this reason, a two-parameter empirical form is used here:

$$C_{\mathrm{P}}(r) = C_{\mathrm{p}}^{\infty}\tanh(r/r_{\mathrm{F}}) \quad (13)$$

where r_{F} expresses the radius at which $C_{\mathrm{P}}(r)$ rapidly approaches the limiting value C_{P}^{∞}. Since coagulation is a function of swollen particle size, the inclusion of this variance of C_{P} with swollen particle size has implications for the particle size distribution: particles that are smaller will swell less than larger particles, which results in slower growth and a greater tendency to coagulate.

The value of V_0, the volume at which precursor particles are formed by either homogeneous or micellar nucleation, is taken to be given by $(4/3)\pi(r_{\mathrm{micelle}})^3$; a sensitivity analysis shows that results are insensitive to the value of V_0 within reasonable bounds.

Conversion and mass conservation. The mass of polymer in the system, m_{p}, is given by:

$$m_{\mathrm{p}} = d_{\mathrm{p}}\int_0^\infty \frac{4}{3}\pi r^3 n(r)\mathrm{d}r \quad (14)$$

The fractional conversion (x) is then obtained from m_{p} and the initial mass of monomer, m_{M}^0:

$$x = \frac{m_{\mathrm{p}}}{m_{\mathrm{M}}^0} \quad (15)$$

In Interval II, the particles are saturated with monomer, and so monomer droplets are present, while in Interval III, no monomer droplets are present and the concentration of monomer in particles and the water phase decreases below their saturation values. In order to determine if the system is in Interval III, the amount of monomer converted to polymer is calculated, and the saturated values of C_{P} and C_{w} (denoted $C_{\mathrm{P}}^{\mathrm{sat}}$ and $C_{\mathrm{w}}^{\mathrm{sat}}$) are used to find the total amount of monomer in the particles and water phase that would be present if the system were in Interval II. If this amount of monomer is less

than the actual amount of monomer in the system, then the system is indeed in Interval II. This is implemented as follows. The mass of polymer in the system is found using equation (14), and the mass of monomer inside the swollen polymer particles (m_s), if the system is in Interval II, is found:

$$m_s = M_0 \int_0^\infty C_P \frac{4}{3}\pi r^3 n(r)\mathrm{d}r \tag{16}$$

For computational simplicity, it is assumed that the size dependence of C_P can be ignored in equation (16), since when the system is indeed in Interval III, the particles are fairly large, when this size dependence is negligible. The mass of monomer in the water phase, m_w, is found using

$$m_w = C_w M_0 V_w \tag{17}$$

where V_w is the volume of the water phase. If $m_p + m_s + m_w$ is less than the starting mass of monomer, then the system is in Interval II. Otherwise the system is in Interval III, and new values of C_P and C_w are calculated iteratively, as follows. In the first iteration, the saturated values are used. At each iteration, a partitioning relation between the saturated and unsaturated values for monomer in the particle and water phases must be used. One such relation is provided by the so-called 'Vanzo' equation[43], but some experimental evidence for its inaccuracy under some circumstances has been put forward[42]. The partitioning relation between saturated and unsaturated monomer in the water and particle phase is taken here to be given by the semi-empirical expression[22,44]:

$$\frac{C_w}{C_w^{sat}} = \left(\frac{C_P}{C_P^{sat}}\right)^{0.6} \tag{18}$$

The mass of monomer in the water phase is then given by equation (17). The mass of monomer swelling the particles is given by:

$$m_s = m_M^0 - m_w - m_p^0 - m_p$$

where m_p^0 is the mass of polymer initially present in the system (as is for the case of a seeded emulsion polymerisation). In the next iteration, a new value of C_P is found from

$$C_P = \frac{m_s}{M_0\left(\frac{m_s}{d_m} - \frac{m_p}{d_p}\right)} \tag{19}$$

This is procedure is repeated until C_P converges to the desired precision.

Micelle concentration and aqueous phase concentrations of surfactant. The absorption of surfactant onto the surface of the latex particles and monomer droplets is assumed to follow the Langmuir adsorption isotherm:

$$A_s = a_s\left(1 + \frac{1}{[S]_w b_s}\right) \tag{20}$$

where a_s is the minimum area which a single surfactant molecule can occupy and A_s is the area actually occupied by a surfactant molecule. The concentration of surfactant in the water phase, $[S]_w$, is related to the number of moles of added surfactant per unit volume of the continuous phase, [S], by

$$[S]_w = [S] - \frac{A_{tot}}{N_A A_S} \tag{21}$$

where A_{tot} is the total surface area of the latex particles:

$$A_{tot} = \int_0^\infty 4\pi n(r) r_s^2 \mathrm{d}r \tag{22}$$

Solving equations (20) and (21) leads to[12]:

$$[S]_w^2 + [S]_w\left(\frac{A_{tot}}{a_s N_A} + \frac{1}{b_s} - [S]\right) - \frac{1}{b_s}[s] = 0 \tag{23}$$

The micelle concentration is then calculated from:

$$[\text{micelle}] = \max\left(0, \frac{[s]_w - cmc}{n_{agg}}\right) \tag{24}$$

where *cmc* is the critical micelle concentration and n_{agg} is the aggregation number for the surfactant.

Rate coefficients

Termination in the aqueous phase. The concentrations of oligomer populations are explicitly calculated for all values of i between 1 and j_{crit}, and the termination rate coefficient is considered to be chain-length dependent[45]. This will yield entry rate coefficients which are a more accurate representation of observed systems. The chain-length dependent termination rate coefficient is calculated using a modification of the Smoluchowski equation for diffusion-controlled reactions[46]:

$$k_{t,w}^{i,j} = 2\pi p_{ij}\sigma_r N_A D_w (i^{-1/2} + j^{-1/2}) \tag{25}$$

where p_{ij} is the spin ratio (expressing the fact that radials must be of opposite spin in order to terminate); σ_r is distance at which the radicals centres are assumed always to react (this is taken as the van der Waals radius of monomer), and D_w is the diffusion coefficient of a monomeric radical in water. The exponent 1/2 for the degree of polymerisation assumes that these short radicals behave like random chains in dilute solution; while there are certainly valid arguments for an exponent closer to unity, the model predictions for particle number and rate are insensitive to this exponent.

Entry and exit rate coefficients. Entry is an important part of the nucleation model,since the fundamental criterion for when particle formation stops or starts is when the rate at which a new radical in the water phase eventually enters a latex particle greatly exceeds that at which it would form a new particle (both events also competing with water-phase termination)[4]. Entry of a radical derived directly from initiator is assumed to occur only for radicals of degree of polymerisation z or greater, while re-entry of an exited radical does not require that the exited propagates first, as set out in equation (9). The entry rate coefficients are in turn assumed to be diffusion-controlled, for which there is experimental evidence[24]. Thus:

$$k_e^i(V) = 4\pi r_s N_A \frac{D_w}{i^{1/2}},\ i \geq z;\ k_e^i(V) = 0,\ i < z \tag{26}$$

$$k_{eE}(V) = 4\pi r_s N_A D_w \tag{27}$$

where an exponent of 1/2 for the diffusion coefficient of small radicals has again been assumed, as in equation (25). Similarly, the rate of entry into a micelle (resulting in one of the two modes of particle formation) is given by:

$$k_{e,\text{micelle}}^i = 4\pi r_{\text{micelle}} N_A \frac{D_w}{i_{1/2}},\ i \geq z;\ k_{e,\text{micelle}}^i = 0,\ i < z \tag{28}$$

where $r_{micelle}$ is the radius of a micelle. As stated, it is likely that equation (26), and perhaps equation (28), require major modification for a system containing electrosteric stabiliser (generated in situ through the presence of a water-soluble co-monomer) or other type of polymeric stabiliser. For exit, $k_{dm} = 3D_w C_w/(c_p r_s^2)$.

Coagulation rate coefficient. We calculate the coagulation rate coefficient between two particles, stabilized by ionic surfactant, using the model of Healy and co-workers[47,48], which is based on the precepts of DLVO theory. The total surface charge on each particle is obtained by adding the charges due to added surfactant and generated charges:

$$\sigma = \sigma_{surf} + \sigma_{gen} \tag{29}$$

The contribution of the ions formed by initiator decomposition at time t is given by:

$$\sigma_{gen} = \frac{2k_d[I]z_+ tN_A e}{A_{tot}} \tag{30}$$

where e is the charge on an electron, z_+ is the counter-ion valence (which is unity for an initiator such as $K_2S_2O_8$), and where it is assumed that all generated surfactant is adsorbed onto the surface of the latex particles. This is an adaptation of the method of Ottewill and co-workers[49]. The surface charge density due to adsorbed surfactant is given by[11]:

$$\sigma_{surf} = \frac{z_+ e}{A_s} \tag{31}$$

The Debye double-layer thickness κ describes the transition of free aqueous-phase ions on the surface of the particles from closely packed to diffuse, and is given by:

$$\kappa = \left(\frac{8\pi N_A I_S e^2}{\varepsilon k_B T}\right)^{\frac{1}{2}} \tag{32}$$

where k_B is Boltzmann's constant, T the temperature, and ε and the ionic strength I_s are defined in the following manner.

$$\varepsilon = 4\pi\varepsilon_0 e_r \tag{33}$$

where ε_0 is permittivity of free space and ε_r is the relative permittivity of water, and

$$I_s = 3[I] + [S] + [Elect] \tag{34}$$

(valid for an initiator such as $K_2S_2O_8$ which is a 1:2 electrolyte, added 1:1 electrolyte of concentration [Elect], and assuming that the surfactant counter-ion is homogeneously distributed).

The surface potential ψ and zeta potential ζ are obtained from the surface charge, using the following expressions. A binary choice function is used to determine the appropriate method of finding the electrostatic potential on the swollen particle[50]. If κr_s is less than 1, then the curvature of the particle surface cannot be ignored and the surface potential is given by:

$$\psi = \frac{4\pi r_s \sigma}{\varepsilon(1+\kappa r_s)} \tag{35}$$

However, if κr_s is greater than 1, the surface of the particle approximates a flat plate, and the surface potential is given by:

$$\psi = \frac{2k_B T}{e}\sinh^{-1}\frac{2\pi e\sigma}{\varepsilon\kappa k_B T} \tag{36}$$

Both expressions take the same value at $\kappa r_s = 1$. The zeta potential of the particles is given by:

$$\zeta = \left(\frac{2k_B T}{z_+ e}\right)\ln\left(\frac{\exp(\lambda_4)+1}{\exp(\lambda_4)-1}\right) \tag{37}$$

$$\lambda_4 = \kappa\delta + \ln\left(\frac{\exp(\lambda_5)+1}{\exp(\lambda_5)-1}\right) \tag{38}$$

$$\lambda_5 = \frac{z_+ e\psi}{2k_B T} \tag{39}$$

where δ is the Stern layer thickness.

The potential between two particles i and j, with swollen radii r_{si} and r_{sj} and centre-to-centre separation R, is given in terms of the Hamaker attractive potential between the two particles[51]:

$$\Phi_A = \frac{-A}{6}\left[\frac{2r_{si}r_{sj}}{R^2-(r_{si}+r_{sj})^2} + \frac{2r_{si}r_{sj}}{R^2-(r_{si}-r_{sj})^2} + \ln\left(\frac{R^2-(r_{si}+r_{sj})^2}{R^2-(r_{si}-r_{sj})^2}\right)\right] \tag{40}$$

where A is the Hamaker constant; the Healy–Hogg–Fursteneau repulsive potential[47] (found by the Derjaguin method[52]) for the repulsive potential between two curved surfaces is:

$$\Phi_R = \frac{\varepsilon r_{si} r_{sj}(\zeta_i^2+\zeta_j^2)}{4(r_{si}+r_{sj})}\left[\frac{2\zeta_i\zeta_i}{\zeta_i^2+\zeta_j^2}\ln\left(\frac{1+e^{-\kappa L}}{1-e^{-\kappa L}}\right) + \ln(1-e^{-2\kappa L})\right] \tag{41}$$

where $L = R - (r_{si} + r_{sj})$. The total potential between the two particles is given by:

$$\Phi = \Phi_A + \Phi_R \tag{42}$$

Once Φ_{max}, the maximum of Φ as a function of inter-particle distance, is found, the coagulation rate coefficient B_{ij} between two particles of swollen radii r_{si} and r_{sj}, equivalent to that between two particles with corresponding unswollen volumes V and V', $B(V,V')$, is then found from the Müller equation[53]:

$$B_{ij} = B_{ji} = \frac{2k_B T}{3\eta W_{ij}}\left(2 + \frac{r_{si}}{r_{sj}} + \frac{r_{sj}}{r_{si}}\right) \tag{43}$$

where η is the viscosity of the medium. The Fuchs stability ratio[49] is found from:

$$W_{ij} = \frac{r_{si}+r_{sj}}{4\kappa r_{si} r_{sj}}\exp\left(\frac{\Phi_{max}}{k_B T}\right) \tag{44}$$

Figure 2 shows the dependence of $B(V,V')$ on the unswollen radii of the two particles, for a system above the cmc, taking the surface coverage to be 100%. It is apparent that the model used here (which is purported to be the best available to calculate coagulation rate coefficients) predicts that very small particles are *always unstable to coagulation*. This arises from the effect of a highly-curved double layer. As discussed elsewhere[12], the inclusion of coagulation of small precursor particles has a significant effect on kinetics, particle size and PSD.

Solution of evolution equations

The equations describing the time evolution of particle size distributions, equations (6)–(8), are solved by finite

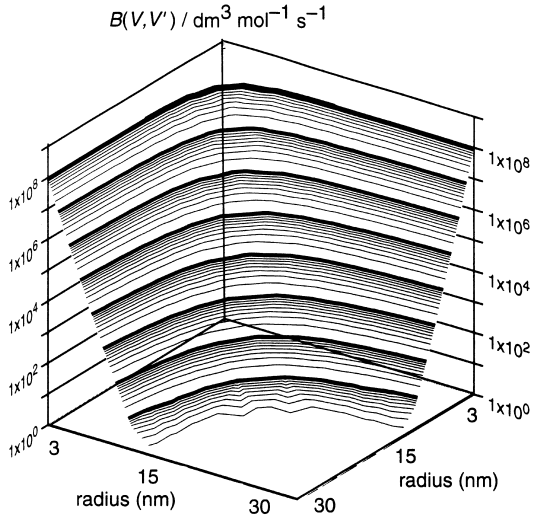

Figure 2 Calculated dependence of $B(V,V')$ on unswollen radii of the two particles, for styrene at 50°C, assuming 100% surface coverage by surfactant; [sodium dodecylsulfate] = 3×10^{-3} mol dm^{-3}, [persulfate] = 10^{-3} mol dm^{-3}

difference, whereby the coupled partial integrodifferential equations in volume and time are converted to a set of coupled ordinary differential equations in terms of time and discrete volume increments. These equations in terms of unswollen volume are in turn converted to corresponding ones in unswollen radius[1], and suitable equal increments of radius Δr (say, $\Delta r = 0.5$ nm) are employed to give a large but manageable number of coupled ordinary first-order differential equations. It is found that accuracy and computational time are both improved by making the steady-state approximation in n_1^M, i.e., in equation (8).

In order to find the contribution to a given size bin (with radius between r_i and $r_i + \Delta r$) from coagulation, a set is found which consists of all the particles size bins which, upon coagulation, will form a particle in the size range r_i. Summing over this set gives the total coagulation rate into bin between r_i and $r_i + \Delta r$.

PARAMETER VALUES FOR STYRENE

The system for which most comparison will be made between theory and model predictions is styrene, with persulfate initiator and sodium dodecylsulfate as surfactant, at 50°C. The parameter values for this system are listed in *Table 1*. Most of these values are taken from the literature, with a few exceptions. The value of r_F was taken as 8 nm, this giving through equation (13) a dependence of C_P on size which is in accord with predictions of the Morton equation with reasonable parameter values.

The *cmc* is often affected by the presence of lipophilic substances such as styrene[54]. The effect of moderate variation in the assumed value of the *cmc* is largely simply to shift the dependence of particle number on surfactant concentration by the same amount in the vicinity of the *cmc*, while values of all observables outside this region remain virtually unaffected[1]. The value for the *cmc* measured for SDS was measured in the absence of styrene using both tensiometry and conductivity as 7.3×10^{-3} mol dm^{-3}, the same as literature value[55,56]. The SDS was purified by conventional liquid–liquid extraction in a Soxhlet apparatus for this purpose. Measuring the *cmc* by conductivity in a styrene emulsion yielded 1.0×10^{-2} mol dm^{-3}.

Table 1 Parameters used in modelling styrene at 50°C

Initiator: persulfate. Surfactant: SDS or AMA.

Quantity	Value	Reference
C_w^{sat}	4.3×10^{-3} mol dm^{-3}	68
C_P^{sat}	5.5 mol dm^{-3}	26
z	3	23
j_{crit}	5	23
A	1×10^{-20} J	69,70
σ_r	5 Å	71
$k_{p,w}$	2.6×10^2 dm^3 mol^{-1} s^{-1}	26
$k_{p,w}^1$	1.2×10^3 dm^3 mol^{-1} s^{-1}	13
$k_{p,w}^2$	2.8×10^2 dm^3 mol^{-1} s^{-1}	13
k_p	2.6×10^2 dm^3 mol^{-1} s^{-1}	26
k_p^1	1.04×10^2 dm^3 mol^{-1} s^{-1}	64
k_{tr}	9.3×10^{-3} dm^3 mol^{-1} s^{-1}	72
D_w	1.5×10^{-5} cm^2 s^{-1}	73
k_d	7.2×10^{-7} s^{-1}	23,74
cmc	3.0×10^{-3} mol dm^{-3} (SDS)	measured by conductivity
	1.0×10^{-2} mol dm^{-3} (AMA)	75
n_{agg}	60	76
a_s	42 Å^2 (SDS); 45 Å^2 (AMA)	77
b_s	2100 dm^3 mol^{-1} (SDS); 1700 dm^3 mol^{-1} (AMA)	77
$r_{micelle}$	2.6 nm	76
V_0	$\pi(r_{micelle})^3$	results insensitive to this value
δ	1.4 Å	10,78
p_{ij}		79
r_F	8 nm	estimated

It is very important to be aware that the values of z and j_{crit} are those applicable to a system with anionic surfactant ($z = 3$, $j_{crit} = 5$). These values were obtained using the following relations[22]:

$$z = 1 + \frac{-23 \text{ kJmol}^{-1}}{RT \ln C_W^{sat}}; \; j_{crit} = 1 - \frac{55 \text{ kJmol}^{-1}}{RT \ln C_W^{sat}} \qquad (45)$$

These relations were obtained semi-empirically, based on free energies of hydration. While the values of z predicted using this expression have been validated for a number of different systems with anionic surfactants[1], there has been no adequate test for the validity of the expression for j_{crit}.

These quantities, and probably the dominant events in radical entry, are very different in systems with any sort of polymeric[57] or electrosteric[58] stabiliser, e.g., in any system containing a water-soluble co-monomer such as acrylic acid, a point to which we return in Section 5.2.

EXPERIMENT

Ab-initio systems

Ab-initio emulsion polymerisations were performed in a batch reactor at 50°C, under slight positive pressure of nitrogen. The monomer used was vacuum distilled at 75°C and used within 24 h of distillation. The water used was purified to Milli-Q standard. Surfactant (sodium dodecylsulfate, SDS) and initiator (potassium persulfate) used were AR Grade (Aldrich).

All components except the initiator were placed in the reactor vessel, under a positive pressure of nitrogen and allowed to thermally equilibrate for approximately 1 h. This procedure should remove most residual oxygen. After this time, the initiator solution was added. Samples were taken at regular intervals, by syringe, and allowed to cool to room temperature. Polymerisation was assumed to cease with exposure to oxygen and cooling to room temperature.

Table 2 Experimental conditions: experiments with no added indifferent electrolyte

[S] (/(mol dm^{-3}))	[I] (/(mol dm^{-3}))
1.0×10^{-3}	1.0×10^{-2}
1.0×10^{-3}	5.0×10^{-3}
1.0×10^{-3}	1.0×10^{-3}
3.0×10^{-2}	1.0×10^{-3}
3.0×10^{-2}	5.0×10^{-3}
3.0×10^{-2}	1.0×10^{-2}
1.0×10^{-2}	5.0×10^{-3}
5.0×10^{-3}	5.0×10^{-3}

Total reaction volume: 1.00 dm^3, mass of monomer: 100 g. Initiator = $K_2S_2O_8$, surfactant = SDS.

Gravimetry was performed on the samples to measure conversion, with samples being dried at 50°C for 12 h, to remove all traces of water and residual monomer.

Particle size distributions were measured using CHDF, with samples removed from the system at intervals throughout the polymerisation, so that changes in the shape of the PSD can be investigated, as can average particle sizes and polydispersity.

The PSDs were obtained over a range of initiator and surfactant concentrations, while other parameters such as temperature and starting monomer concentrations were kept constant. *Table 2Table 3* list the experimental conditions.

Experiments were performed with added 1:1 electrolyte, to investigate any effects of coagulation above the critical micelle concentration. Similar experiments have been performed below the critical micelle concentration by Ottewill and co-workers[59,60].

Reproducibility of the experimental results are good, with particle numbers varying by less than 5% in duplicate experiments above the *cmc*. Reproducibility of the particle sizes at low surfactant concentrations was not investigated.

In addition to data obtained as above for SDS, comparison was also made with observed particle number as a function of concentration of Aerosol MA80 (AMA, sodium dihexylsulfosuccinate)[1,61].

Seeded systems: amount of secondary nucleation

Comparison was also made with previously-published data from a series of seeded emulsion polymerisations of styrene wherein the amount of secondary nucleation was measured by calibrated electron microscopy; experimental details have been published elsewhere[4]. These data were for the relative number of new particles formed when initial number concentration and particle size were varied against a constant surfactant concentration (8×10^{-4} mol dm^{-3} SDS) and initiator concentration (1.2×10^{-3} mol dm^{-3} persulfate) for a seeded homopolymerisation of styrene. The surfactant concentration was chosen to be below the critical micelle concentration for the surfactant, so that micellar entry need not be considered.

RESULTS

Ab initio systems

Particle number. Figures 3–7 compare predicted and observed particle number as a function of variations in surfactant and initiator concentration, and as a function of ionic strength. The origin of the overall sigmoidal shape of the variation of N_c with surfactant concentration seen in the calculations (and possibly, although not definitively, seen in experiment) is well understood: it arises as the systems changes from nucleation exclusively by homogeneous nucleation to dominance by micellar nucleation well above the *cmc*.

It can be seen in each case that the model reproduces experiment adequately, but imperfectly. One effect that is not successfully reproduced is the variation of N_c with surfactant concentration at about the *cmc*: the model predicts a very rapid change, while experiment shows that this is in actuality much more gradual. As also discussed in Section 5.3, the position of the rapid drop-off predicted by the model depends on the value assumed for the *cmc*, which is known in turn to depend on the presence of monomer and on the ionic strength. However, whatever the assumed value of the *cmc*, the present model,and simpler variants of it[1,11,12], always predict a much more sudden rise in N_c at the *cmc* than is seen experimentally. This qualitative lack of accord between model and experiment can be ascribed to the assumption in the model that micelles are completely absent below the *cmc*; in actuality, micelle-like entities are probably formed transiently just below the *cmc* and these

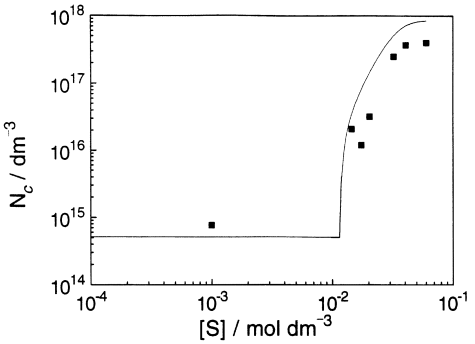

Figure 3 Comparison between observed and predicted particle number for styrene, with varying Aerosol MA80 concentration while persulfate concentration is held at 1.3×10^{-2} mol dm^{-3}; no added electrolyte. Points: experiment[1,61] above the *cmc*; zero-surfactant value (given on the plot as at 10^{-4} mol dm^{-3} surfactant) calculated from interpolation formulae given by Goodwin *et al.*[60] based on experimental data for similar conditions. Line: calculated

Table 3 Experimental conditions: experiments with varying initiator concentration but constant ionic strength (added NaCl)

[S] (/(mol dm^{-3}))	[I] (/(mol dm^{-3}))	[NaCl] (/(mol dm^{-3}))	Ionic strength (/(mol dm^{-3}))
1.0×10^{-2}	1.0×10^{-2}	0	4.0×10^{-2}
1.0×10^{-2}	5.0×10^{-3}	1.0×10^{-2}	3.5×10^{-2}
1.0×10^{-2}	5.0×10^{-3}	1.5×10^{-2}	4.0×10^{-2}
1.0×10^{-2}	1.0×10^{-3}	2.7×10^{-2}	4.0×10^{-2}
1.0×10^{-2}	5.0×10^{-3}	0	2.5×10^{-2}
1.0×10^{-2}	5.0×10^{-3}	2.7×10^{-2}	5.2×10^{-2}
1.0×10^{-2}	5.0×10^{-3}	1.0×10^{-1}	1.3×10^{-1}

Total reaction volume: 1.00 dm^3, mass of monomer: 100 g. Initiator = $K_2S_2O_8$, surfactant = SDS.

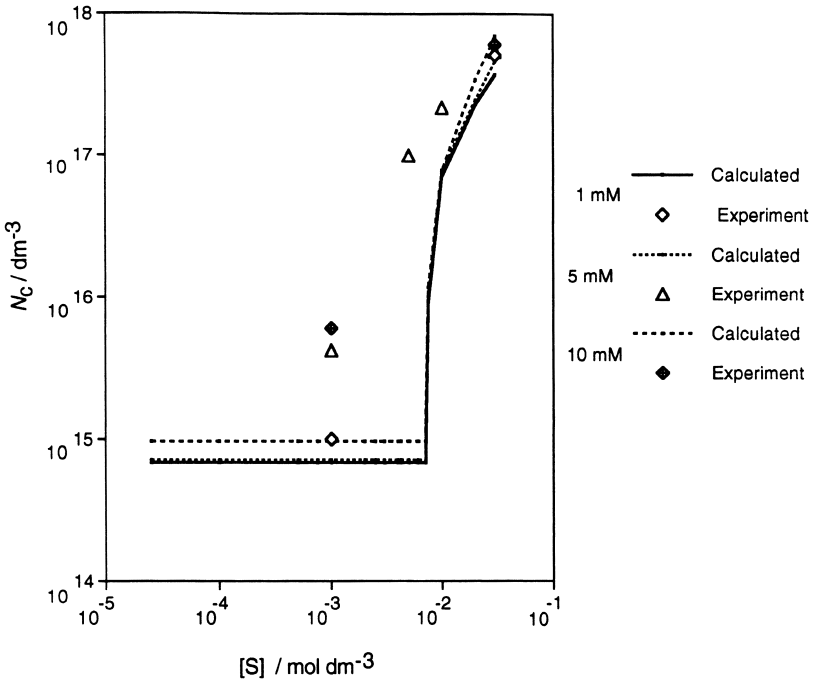

Figure 4 Comparison between observed and predicted particle number for styrene, with varying SDS concentration while persulfate concentration is held constant at 1.0×10^{-3} mol dm^{-3}; no added electrolyte

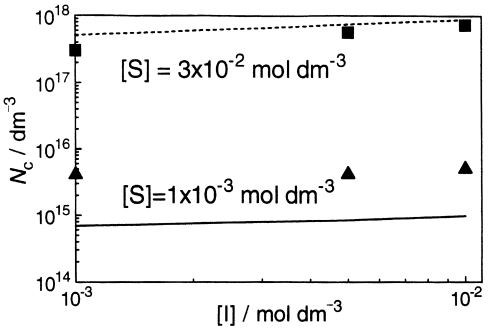

Figure 5 As in *Figure 4*, except that initiator concentration is varied while SDS concentration is held fixed at either 1.0×10^{-3} or 3×10^{-2} mol dm^{-3}

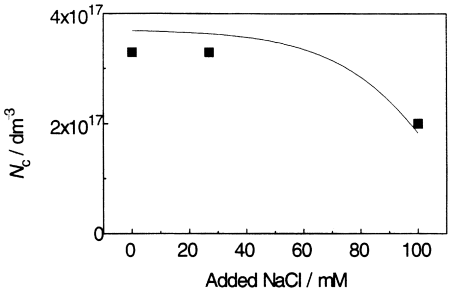

Figure 6 As in *Figures 4 and 5*, except that [persulfate] $= 5 \times 10^{-3}$ mol dm^{-3}, [SDS] $= 1 \times 10^{-2}$ mol dm^{-3}, while the amount of added electrolyte (NaCl) was varied

could act as loci for nucleation, thereby smoothing the sharp change predicted by the model.

It is especially important to note the successful prediction of the effect of indifferent electrolyte somewhat above the *cmc*, which results in a significant change in particle number, seen in *Figure 6*. This must be due to coagulation of small particles, which the model predicts to be a significant kinetic event[12]. The change with concentration of indifferent electrolyte seen experimentally is unlikely to be due to changes in the *cmc* caused by the change in ionic strength, since the model is completely insensitive to the value of the *cmc* at these surfactant concentrations.

Figure 7 shows data for the dependence on initiator concentration whereby the effects of changing ionic strength have been eliminated through addition of appropriate amounts of NaCl (*Table 2*) to keep ionic strength constant while initiator concentration is changed; this eliminates any effects on particle number due to the ionic strength changing while initiator concentration is changed (the change in ionic strength would change the coagulation rate coefficients). It can be seen that acceptable accord is obtained. Note that the slope of the experimental and calculated dependences of logN_c on log[initiator] are 0.25 and 0.23 respectively; this can be compared with the classical Smith–Ewart value of 0.4. When there is no added electrolyte to keep the ionic strength constant, the experimental and calculated exponents become 0.20 and 0.21

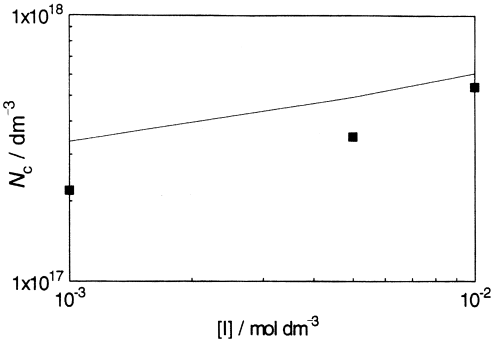

Figure 7 As in *Figures 4–6* except that the ionic strength is kept constant at 4.0×10^{-3} mol dm^{-3} while initiator concentration is varied (data from *Tables 2 and 3*)

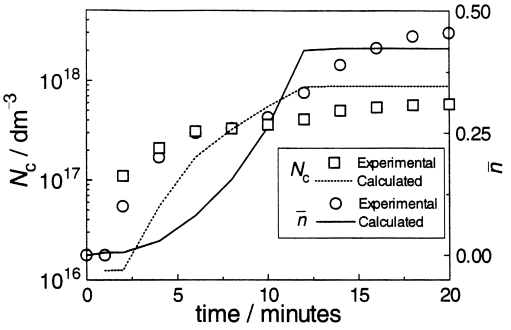

Figure 8 Experimental and observed dependence of particle number and of $\bar{n}$ as a function of time for [persulfate] $= 5 \times 10^{-3}$ mol dm^{-3}, [SDS] $= 3 \times 10^{-2}$ mol dm^{-3}

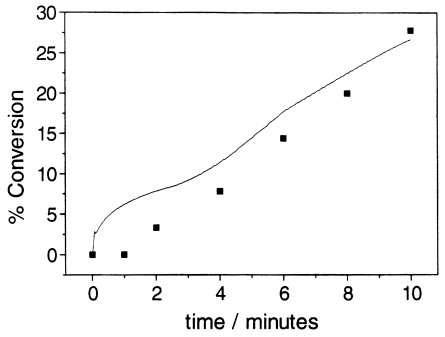

Figure 9 Comparison of observed and predicted time dependence of conversion with [persulfate] $= 5 \times 10^{-3}$ mol dm^{-3}, [SDS] $= 3 \times 10^{-2}$ mol dm^{-3}

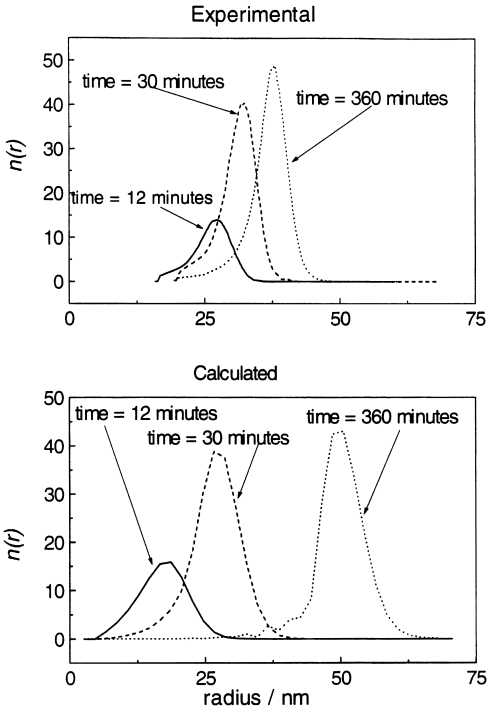

Figure 10 Experimental (full lines) and calculated (broken lines) particle size distributions for [SDS] $= 3 \times 10^{-2}$ mol dm^{-3}, [persulfate] $= 5 \times 10^{-3}$ mol dm^{-3} at 6, 30 and 360 min. Distributions at each time have been normalised to conversion

respectively. This shows that there is a small but significant effect of coagulation, and at the same time emphasises that the Smith–Ewart model should be regarded as qualitative rather than quantitative.

Below the *cmc*, the agreement between model and experiment is quite poor, with particle number being significantly underestimated. The sensitivity analysis discussed in Section 5.3 suggests that this may be ascribed to uncertainties in the value of j_{crit} (while of course the model predictions are insensitive to j_{crit} above the *cmc*) and in the model for the coagulation rate coefficients.

While the dependences of particle number on surfactant and initiator concentrations above the *cmc* are in qualitative accord with the simple Smith–Ewart predictions that $N_c \propto [I]^{0.4}[S]^{0.6}$, this is of course not the case near and below the *cmc*; moreover, the Smith–Ewart exponents are only obeyed over a small range[62,63].

Rate. *Figure 8* compares calculated and observed particle number and $\bar{n}$ as functions of time for $[S_2O_8^{2-}] = 5 \times 10^{-3}$ mol dm^{-3}, [SDS] $= 3 \times 10^{-2}$ mol dm^{-3}. Except at very early times when data are inaccurate, it is seen that the model reproduces the observed behaviour of $N_c(t)$ quite well, but the predicted form of $\bar{n}$ is not accurately reproduced. While the final value of $\bar{n}$ is predicted with acceptable accuracy, it is seen that the model actually predicts the wrong *shape* for the time dependence of this quantity: the experimental result shows a concave-down dependence, while the model predicts a concave-up behaviour. The reason for this is not apparent at this stage.

Figure 9 compares observed and predicted conversion/time curves during the period of particle formation. The rate is of course the product of particle number and $\bar{n}$, and thus incorporates discrepancies in both quantities shown in *Figure 8*—and it must be kept in mind that accord between predicted and experimental rate can arise from cancellation of errors in calculated N_c and $\bar{n}$! The predicted rate curves are sensitive to the rate coefficient for propagation, within the particle, of a monomeric radical formed by transfer (k_p^1), which has a strong effect on k_{dM} and hence on exit[64]. The value of 1.04×10^2 dm^3 mol^{-1} s^{-1} estimated from independent measurements (γ-radiolysis relaxation in a seeded system)[64] gives acceptable accord with the present rate data for this ab initio system.

Particle size distributions. It has been noted that the shape of the early-time particle size distribution in an ab initio emulsion polymerisation is sensitive to assumptions as to the mechanisms of particle formation[2]. *Figure 10* shows the observed and predicted PSDs as functions of unswollen radius, for the same set of calculated and experimental times. At first sight the accord is poor, but that is at least in part due to the imperfections in the model's predictions of particle number and conversion as distinct from any failings in predicting the shape of the PSD. *Figure 11* shows experimental and predicted size distributions at the same conversions (rather than at the same times), and it can be seen that now the general shape predicted by the model is correct.

It has been stated[2] that PSDs obtained by electron microscopy in samples taken at early times (just after particle formation has finished), when plotted as the volume distribution $n_V(V)$, exhibit a *characteristic positive skewness* (this was originally taken as evidence for the occurrence of coagulation during particle formation, although it is now considered that, while coagulation is indeed likely, these data do not provide such evidence[24]). *Figure 12* shows the early-time PSDs of *Figure 11* replotted as volume distributions, using equation (11). It can be seen

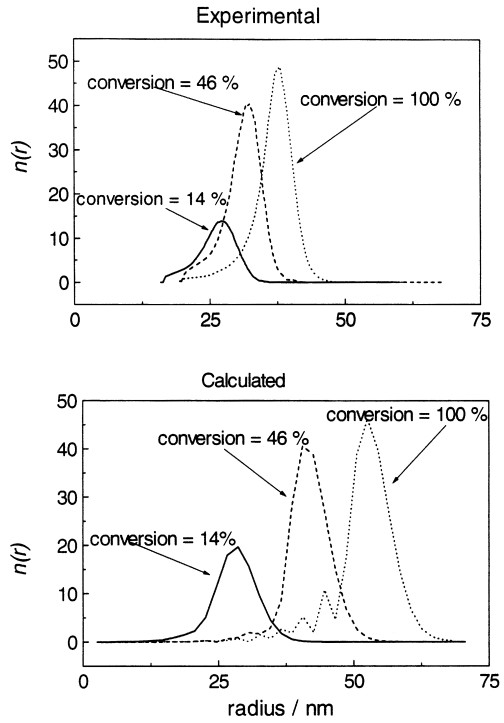

Figure 11 Experimental (full lines) and calculated (broken lines) particle size distributions for run of *Figure 10* at 14, 46 and 100% conversions (corresponding to the conversions at the experimental times of *Figure 10*)

that the positive skewness reported in PSDs obtained by electron microscopy[2,65] is *not particularly apparent either in experiment or in modelling*. The overall shape of the volume distributions obtained experimentally and from modelling are in qualitative accord, including the lack of a very pronounced positive skewness (although some positive skewness is apparent in both).

The discrepancy in skewness between the two sets of experimental data may be due to artifacts or biases in PSDs of very small particles measured by different experimental techniques (AUC and electron microscopy). The lack of pronounced skewness in the calculated volume distribution is due to the proper inclusion of compartmentalisation: i.e., explicitly modelling n_0, n_1^M and n_1^P in the evolution equations coupled with assuming a physically realistic increase of monomer concentration with increasing particle size.

Secondary nucleation

In order to calculate the amount of secondary nucleation, an initial distribution was calculated from the number

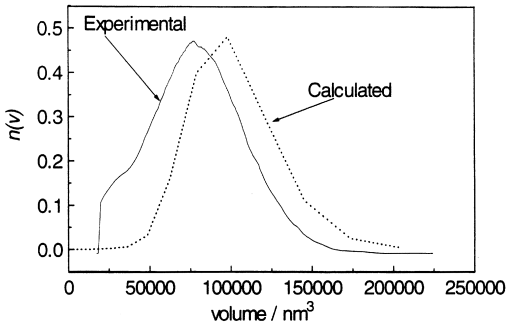

Figure 12 Particle size distribution data at 12 minutes re-plotted as volume distributions (equation (11))

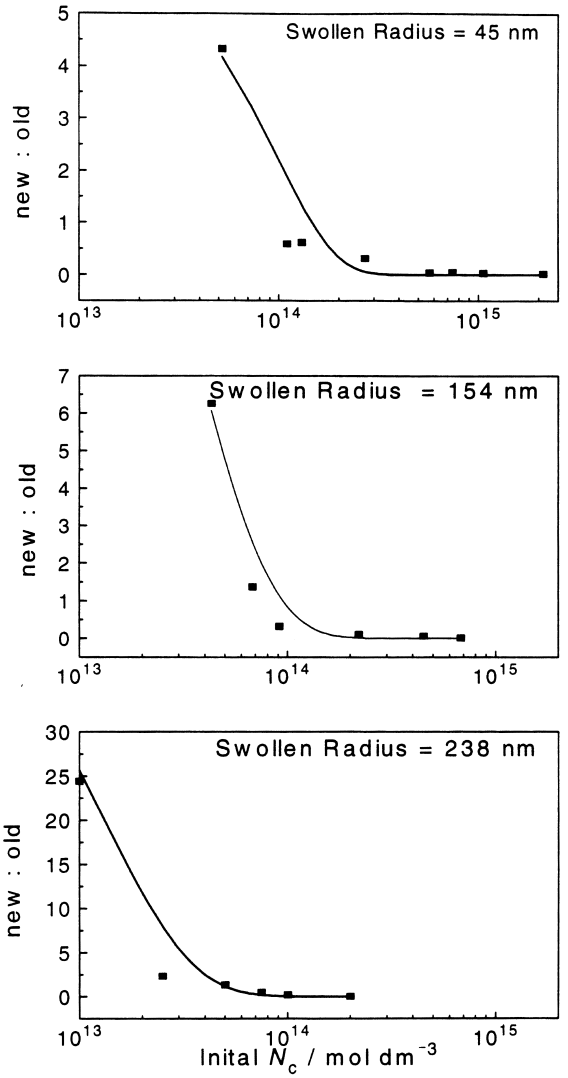

Figure 13 Predicted (lines) and observed[4] (points) relative amounts of secondary nucleation (as ratio of new to old particle number concentrations) for styrene seeded emulsion polymerisation with various particle sizes and concentration. The surfactant is 8×10^{-4} mol dm^{-3} sodium dodecylsulfate (SDS) and the initiator is 1×10^{-3} mol dm^{-3} potassium persulfate

concentration of particles, average radius and polydispersity. The surface charge density on the seed particles was assumed to be equivalent to 0.3 C m^{-2}, which is the surface charge when the surface is totally covered by surfactant. There was no information available on the polydispersity of the seed particles, so a polydispersity of 1.05 was used. The final particle number of new particles was found not to be sensitive to polydispersity within a range of physically reasonable polydispersity values.

As can be seen in *Figure 13*, the model is very successful at predicting the relative amounts of secondary nucleation, over a range of seed particle sizes, and starting number concentration of particles. This same success was seen, although with less quantitative accuracy, in an earlier, more primitive, treatment[4].

Sensitivity analysis

With a model as complex as the present one, it is essential to perform an analysis to see to which parameters the final results are sensitive: inferences drawn from agreement or disagreement with experiment will obviously depend on whether or not such agreement can be altered with changes of input parameter values within reasonable limits. The

benchmark calculations used for this sensitivity analysis were low and high surfactant concentrations (1×10^{-3} and 3×10^{-2} mol dm^{-3}, below and well above the *cmc* for SDS), 1×10^{-3} mol dm^{-3} persulfate, and the quantities examined were the particle number after 20 min (when particle formation is essentially finished), and the rate of particle formation, which is dN_c/dt at $t = 2$ minutes, which typifies the period of extensive particle formation (as exemplified in *Figure 8*). For this sensitivity analysis, the following parameters were varied.

- The minimum area which a single surfactant molecule occupies, a_s, which was increased from 42 to 63 Å. Coagulation events may be affected by this parameter, as will surfactant coverage and hence the point at which micelles disappear.
- The radius of a micelle, $r_{micelle}$, was reduced from 2.6 nm to 2 nm and increased to 5.6 nm; this parameter of course could only affect the system above the *cmc*. This parameter would affect particle number if the actual entry into a micelle is rate-determining, rather than the micelles acting only as monomer-rich loci for polymerization and as surfactant reservoirs.
- The way that surfactant counter-ion affects ionic strength I_s, which in the normal treatment is found as 3[I] + [S] + [Elect] (equation (35)); this was found alternatively (a) as 3[I] + 0.5[S] + [Elect], and (b) as 3[I] + [Elect]. Coagulation events may be affected by these changes.
- The quantity r_F which gives the dependence of monomer concentration on particle size (equation (13)), which was increased from 8 nm to 12 nm. This will affect how quickly a precursor particle can grow by propagation.
- The propagation rate coefficient of monomeric radicals in the water phase, $k^1_{p,w}$, which was halved from its standard value. This may affect the entry rate if this first step, involved for example in equation (1), is slow enough to be rate-determining; under these circumstances this will affect the rate of growth of precursor particles.
- The value of the rate coefficient for transfer to monomer, k_{tr}, was doubled. This will affect the exit rate, and hence the rate of growth of precursor particles.
- The propagation rate coefficient in the particle phase, k^1_p, which was halved from its standard value. This will also affect the exit rate, and hence the rate of growth of precursor particles.
- The value of j_{crit} (which was taken as 5 in the standard calculation) was taken as 4 and as 6. This will affect the rate of particle formation by homogeneous nucleation (which only is significant below the *cmc*).

Other quantities in the model are felt to be such that no significant variation is reasonable: for example, the value of *z* cannot be varied since it was chosen to give accord with extensive data on entry in seeded systems. Although not illustrated here, it has been shown elsewhere[1] that the effect of changing the *cmc* is essentially just to change the position of the rapid decrease in N_c with [S]. Other parameters for which no sensitivity analyses are shown are quantities such as n_{agg}, for which it has been shown[1] that models of this type are insensitive, for the same reason (given below) that the model predictions will be seen to be insensitive to the value of $r_{micelle}$.

The results of these variations are shown in *Figure 14*, as ratios of particle number and rate to those of the 'benchmark' sets. It can be seen that, at least for this particular set of 'benchmark' parameters, the model predictions for

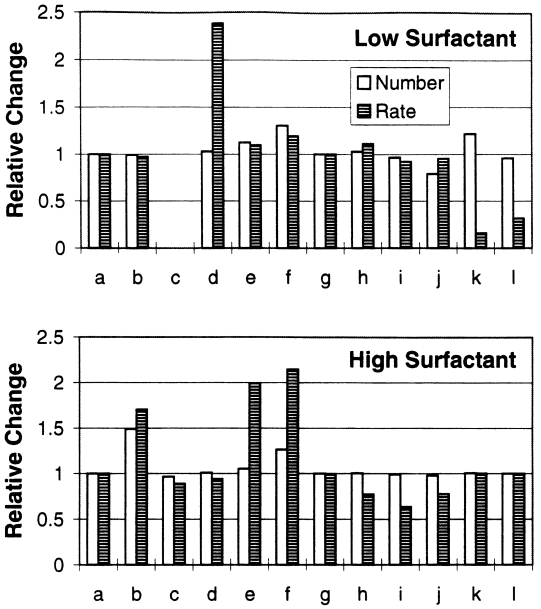

Figure 14 Sensitivity analysis, showing the relative changes in particle number, N_c(changed)/N_c(benchmark), and in nucleation rate, [dN_c(changed)/dt]/[dN_c(benchmark)/dt], for parameter changes, for high and low surfactant concentrations. a) 'baseline' (*Table 1*); b) a_s increased by 50% (63Å); c) $r_{micelle}$ decreased to 2 nm; d) $r_{micelle}$ increased to 5.6 nm; e) ionic strength calculated from 3[I] + [E] + 0.5[S]; f) ionic strength calculated from 3[I] + [E]; g) r_F increased by 50% to 12 nm; h) $k^1_{p,w}$ halved to 700 dm^3 mol^{-1} s^{-1}; i) k^1_p halved to 700 dm^3 mol^{-1} s^{-1}; j) k_{tr} doubled to 0.06 dm^3 mol^{-1} s^{-1}; k) $j_{crit} = 4$; l) $j_{crit} = 6$

particle number are remarkably insensitive to most of these parameter variations, although the rate at which this particle number is attained does vary. Above the *cmc*, the only significant sensitivity is to a_s, while below the *cmc*, the most significant sensitivity is to j_{crit}.

These results can be readily understood through the so-called ''fundamental criterion for particle formation''[4]: that particle formation stops (or starts, for secondary nucleation) when the rate at which a newly-formed water-phase radical enters a pre-existing particle exceeds that at which it undergoes nucleation (by either micellar or homogeneous nucleation). Consider the high-surfactant situation; the value of N_c at which nucleation ceases can be considered as being governed by when plots of these two rates (entry and micellar nucleation) intersect, when each is plotted as a function of N_c. The sensitivity to a_s (the area occupied by a surfactant molecule at saturation) and insensitivity to other parameters arises because of surfactant coverage. The rate of *entry* is essentially $k_{p,w}[IM^\bullet_z]N_c$ (equation (9)), which will not be affected by $k^1_{p,w}$ if the first propagation step is very fast, and will be independent of all other parameters which are varied in this sensitivity analysis for a given value of N_c. The rate at which a radical can form a new particle by *micellar nucleation* falls from finite to zero as micelles disappear. This will happen when the particle surface becomes sufficiently covered with surfactant: effectively the elementary Smith–Ewart notion.

The value of N_c at which this coverage occurs is of course sensitive to a_s. The Smith–Ewart treatment[9] predicts a dependence of $a_s^{3/5}$; the present model gives a dependence of $a_s^{0.78}$. How will N_c vary with the other parameters in the sensitivity analysis? The rate at which sufficient particle surface is formed to adsorb all surfactant is relatively insensitive to r_F because this affects propagational growth only very early on, while most of the surface area in the

system is from larger particles ($area \propto r_s^2$) wherein the monomer concentration takes on its limiting value. The insensitivity to $r_{micelle}$ is simply because the actual event of entry into a micelle is so fast as not to be rate-determining. There is a slight dependence on the inclusion of counterions in the ionic strength, because coagulation changes particle surface area without changing conversion. There is no sensitivity to the parameters which govern the exit rate coefficient, viz., k_p^1 and k_{tr}, because for this particular system, the value of $\bar{n}$ was very close to $\frac{1}{2}$ (and thus the particle growth kinetics are insensitive to exit). Under these circumstances, the rate at which particles grow once formed is independent of most parameters except coagulation. Then particles of a given N_c always have same total area (except for coagulation effects) independent of other parameters. As stated, the nucleation rate plummets when sufficient surfactant is adsorbed for micelles to disappear; this will always happen at same N_c for each parameter set, since the growth rate will always be the same. Since the model for entry used here is such that the entry rate is approximately proportional to N_c and independent of other parameters which are varied in this sensitivity analysis[23], the entry rate and nucleation rate curves will always intercept at same N_c for different parameter sets.

Given the insensitivity of the final particle number to the parameters whose values are deemed uncertain, the explanation for the poor accord with experimental particle number below the *cmc* is not apparent. Two explanations are:

(1) that this is due to inaccuracies in the model for coagulation, and
(2) the value of j_{crit} is not correct. This is an area of further work.

PREDICTIONS OF THE EFFECT OF POLYMERIC STABILISER

It has been observed that the mechanism for entry and exit used here becomes invalid for systems containing polymeric stabiliser: the rate coefficients for both processes are dramatically less than what is seen in an otherwise essentially identical system with anionic stabiliser[58]. This is likely to have a pronounced effect on secondary particle formation, in view of the fundamental criterion for particle formation stopping or starting, viz., that a new radical formed in the water phase becomes much more likely to enter a pre-existing particle than to form a new one [4]. *Figure 15* shows a model calculation where this effect was imitated in the present system by increasing z to an 'effective' value of 10 (compared to its value of 3 for styrene with ionic stabiliser). It can be seen that secondary nucleation is predicted to be much more pronounced. This is in quantitative accord with the qualitative prediction from this criterion for the effect of polymeric stabiliser on secondary particle formation: the reduced entry rate coefficient that arises from an increased value of z will mean that a new radical is more likely to undergo secondary particle formation. This inference is in accord with many experimental observations (e.g.,[66,67]) that secondary nucleation is increased in systems containing polymeric stabiliser.

CONCLUSIONS

The model given here proves a satisfactory accord with experiment for a wide range of observables which are sensitive to particle formation mechanisms in styrene emulsion polymerisations.

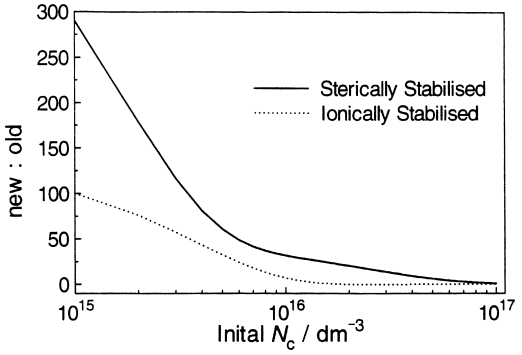

Figure 15 Illustrating the effect of polymeric surfactant on secondary particle formation: calculated relative amounts of secondary nucleation with [persulfate] = 10^{-3} mol dm^{-3}, [sodium dodecylsulfate] = 2×10^{-2} mol dm^{-3}

Experiments show that the effect of coagulation of newly-formed (precursor) particles is significant even above the critical micelle concentration, despite the stabilizing effect of the surfactant, i.e. when the addition of 100 mM of NaCl leads to a decrease in the particle number by a factor of one third. This large effect cannot be ascribed to a change in the *cmc* induced by the added electrolyte (although of course this change will take place), since the model strongly suggests that changing the *cmc* has no significant effects on observables as long as the system is well above or below the *cmc*. Another effect which the model explains is the general observation that secondary nucleation occurs readily in systems stabilised with polymeric surfactant, since the experimental observation that such surfactants reduce the rate of entry into latex particles then suggests that radicals which are unable to enter may instead form new particles.

At least for a system such as styrene, there are very few parameters whose values are not available from independent measurements. Those values for styrene whose parameters are uncertain have only slight effects on the predictions of the model.The fact that accord is imperfect but adequate suggests that the model can be used predictively for other systems, especially with regard to the onset of secondary nucleation. However, it must be emphasized that, even for styrene, there are still many uncertainties: for example, the large effect of electrosteric and other polymeric stabilisers (e.g., in systems with water-soluble co-monomers such as acrylic acid) on the parameters controlling entry[58], the value of j_{crit} and the model used for coagulation.

ACKNOWLEDGEMENTS

The generous support of, and stimulating scientific discussions with, Dr Dieter Diestler of BASF are gratefully acknowledged, as is partial support by the Australian Research Council.

REFERENCES

1. Gilbert, R. G. *Emulsion Polymerization: A Mechanistic Approach.* Academic, London, 1995.
2. Lichti, G., Gilbert, R. G. and Napper, D. H., *J. Polym. Sci. Polym. Chem. Edn*, 1983, **21**, 269.
3. Hansen, F. K. and Ugelstad, J, *J. Polym. Sci. Polym. Chem. Edn*, 1979, **17**, 3047.

4. Morrison, B. R. and Gilbert, R. G., *Macromol. Symp.*, 1995, **92**, 13.
5. Dos Ramos, J. G. and Silebi, C. A., *Polym. Int.*, 1993, **30**, 445.
6. Priest, W. J., *J. Phys. Chem.*, 1952, **56**, 1077.
7. Fitch, R. M., and Tsai, C. H. In *Polymer Colloids*, ed. Fitch, R. M.. Plenum, New York, 1971, p. 73.
8. Ugelstad, J. and Hansen, F. K., *Rubber Chem. Technol.*, 1976, **49**, 536.
9. Smith, W. V. and Ewart, R. H., *J. Chem. Phys.*, 1948, **16**, 592.
10. Feeney, P. J., Napper, D. H. and Gilbert, R. G., *Macromolecules*, 1987, **20**, 2922.
11. Richards, J. R., Congalidis, J. P. and Gilbert, R. G., *J. Appl. Polym. Sci.*, 1989, **37**, 2727.
12. Coen, E. M., and Gilbert, R.G., in: *Polymeric Dispersions. Principles and Applications*, ed. Asue, J.M. Vol. NATO Advanced Studies Institute. Kluwer Academic, Dordrecht, 1997, p. 67.
13. Casey, B. S., Morrison, B. R. and Gilbert, R. G., *Progr. Polym. Sci.*, 1993, **18**, 1041.
14. Giannetti, E., *Macromolecules*, 1990, **23**, 4748.
15. Schlüter, H., *Colloid Polym. Sci.*, 1993, **271**, 246.
16. Schlüter, H., *Macromolecules*, 1990, **23**, 1618.
17. Hansen, F. K. and Ugelstad, J., *J. Polym. Sci. Polym. Chem. Edn*, 1978, **16**, 1953.
18. Fitch, R. M., Palmgren, T. H., Aoyagi, T. and Zuikov, A., *Angew Makromol. Chemie (Vol. 123–124)*, 261, 1984.
19. Hansen, F. K., *Chem. Eng. Sci.*, 1993, **48**, 437.
20. Litt, M., Patsiga, R. and Stannett, V., *J. Polym. Sci. Part A-1*, 1970, **8**, 3607.
21. Starnes, W. H., Chung, H. and Benedikt, G. M., *Polym. Preprints*, 1993, **34**, 604.
22. De Bruyn, H., Gilbert, R. G. and Ballard, M. J., *Macromolucules*, 1996, **29**, 8666.
23. Maxwell, I. A., Morrison, B. R., Napper, D. H. and Gilbert, R. G., *Macromolecules*, 1991, **24**, 1629.
24. Morrison, B. R., Maxwell, I. A., Gilbert, R. G., Napper, D. H., in *ACS Symp. Series - Polymer Latexes - Preparation, Characterization and Applications*, ed. ES Daniels, ED Sudol, M El-Aasser. Vol. 492. American Chemical Society, Washington, DC, 1992, p. 28.
25. Gilbert, R. G., in *Emulsion Polymerization and Emulsion Polymers*, ed. Lovell, P. A. and El-Aasser, M. S. Wiley, London, 1997, p. 165.
26. Hawkett, B. S., Napper, D. H. and Gilbert, R. G., *J. Chem. Soc. Faraday Trans. 1*, 1980, **76**, 1323.
27. Ugelstad, J., Mørk, P. C., Dahl, P. and Rangenes, P., *J. Polym. Sci. Part C*, 1969, **27**, 49.
28. Nomura, M. and Harada, M., *J. Appl. Polym. Sci.*, 1981, **26**, 17.
29. Nomura, M., Harada, M., Nakagawara, K., Eguchi, W. and Nagata, S., *J. Chem. Eng. Japan*, 1970, **4**, 160.
30. Maruthamuthu, P., *Makromol. Chem. Rapid Commun.*, 1980, **1**, 23.
31. McAskill, N. A. and Sangster, D. F., *Aust. J. Chem.*, 1979, **32**, 2611.
32. McAskill, N. A. and Sangster, D. F., *Aust. J. Chem.*, 1984, **37**, 2137.
33. Koltzenburg, G., Bastian, E. and Steenken, S., *Angew Chem. Int. Edn Engl.*, 1988, **27**, 1066.
34. Neta, P., Huie, R. E. and Ross, A., *J. Phys. Chem. Ref. Data*, 1988, **17**, 1027.
35. Clifton, C. L. and Huie, R. E., *Int. J. Chem. Kinet.*, 1989, **21**, 677.
36. Heuts, J. P. A., Radom, L. and Gilbert, R. G., *Macromolecules*, 1995, **28**, 8771.
37. Lichti, G., Hawkett, B. H., Gilbert, R. G., Napper, D. H. and Sangster, D. F., *J. Polym. Sci. Polym. Chem. Edn*, 1981, **19**, 925.
38. Morton, M., Kaizerman, S. and Altier, M. W., *J. Colloid Sci.*, 1954, **9**, 300.
39. Gardon, J. L., *J. Polym. Sci. Part A-1*, 1968, **11**, 2859.
40. Ugelstad, J., Mørk, P. C., Mfutakamba, H. R., Soleimmany, E., Nordhus, I., Schmid, R., Berge, A., Ellingsen, T., Aune, O. and Nustad, K., in *Science and Technology of Polymer Colloids: Preparation and Reaction Engineering*, ed. Poehlein, GW, Ottewill, RH, and Goodwin, JW. Vol. 1. Martinus Nijhoff Publishers, Boston, MA, 1983, p. 51.
41. Antonietti, M., Kaspar, H. and Tauer, K., *Langmuir*, 1996, **12**, 6211.
42. Kukulj, D. and Gilbert, R. G., in: *Polymeric Dispersions. Principles and Applications*, ed. Asua, JM. NATO Advanced Studies Institute. Kluwer Academic, Dordrecht, 1997, p. 97.
43. Vanzo, E., Marchessault, R. H. and Stannet, V., *J. Colloid Sci.*, 1965, **20**, 62.
44. Maxwell, I. A., Kurja, J., van Doremaele, G. H. J., German, A. L. and Morrison, B. R., *Makromol. Chem*, 1992, **193**, 2049.
45. Russell, G. T., Gilbert, R. G. and Napper, D. H., *Macromolecules*, 1992, **25**, 2459.
46. Russell, G. T., Gilbert, R. G. and Napper, D. H., *Macromolecules*, 1993, **26**, 3538.
47. Hogg, R., Healy, T. W. and Furstenau, D. W., *Trans Faraday Soc.*, 1966, **62**, 1638.
48. Wiese, G. R. and Healy, T. W., *Trans Faraday Soc.*, 1970, **66**, 490.
49. Ottewill, R. O., in: *Emulsion Polymerization*, ed. Piirma, I. Academic, New York, 1982, p. 1.
50. Overbeek, J. T. G., in: *Colloid Science* ed. Kruyt, HR. Elsevier, Amsterdam, 1960.
51. Hamaker, H. C., *Physica*, 1937, **4**, 1058.
52. Derjaguin, B. V., Krotova, N. A., Karassev, V. V., Kirillova, Y. M. and Aleinikova, I. N., *Prog Surface Sci*, 1994, **45**, 95.
53. Müller, H., *Kolloid-Beih*, 1928, **26**, 257.
54. Rosen, M. J. *Surfactants and Interfacial Phenomena*. Wiley, New York, 1978.
55. Elworthy, P. H. and Mysels, K. J., *J. Coll. Sci.*, 1996, **21**, 331.
56. Flockhart, B. D., *J. Coll. Sci.*, 1961, **16**, 484.
57. Kusters, J. M. H., Napper, D. H., Gilbert, R. G. and German, A. L., *Macromolecules*, 1992, **25**, 7043.
58. Coen, E., Lyons, R. A. and Gilbert, R. G., *Macromolecules*, 1996, **29**, 5128.
59. Ottewill, R. H., in: *Future Directions in Polymer Colloids* ed. El-Aasser, M. S., and Fitch, R. M. Martinus Nihoff, Dordrecht, 1987.
60. Goodwin, J. W., Hearn, J., Ho, C. C. and Ottewill, R. H., *Colloid Polym. Sci.*, 1974, **252**, 464.
61. Hidi, P., unpublished data.
62. Fitch, R. M., *Brit. Polym. J.*, 1973, **5**, 467.
63. Gardon, J. L., *J. Polym. Sci. Part A-1*, 1968, **11**, 643.
64. Morrison, B. R., Casey, B. S., Lacík, I., Leslie, G. L., Sangster, D. F., Gilbert, R. G. and Napper, D. H., *J. Polym. Sci. A Polym. Chem.*, 1994, **32**, 631.
65. Feeney, P. J., Napper, D. H. and Gilbert, R. G., *J. Colloid Interface Sci.*, 1987, **118**, 493.
66. Lepizzera, S. M. and Hamielec, A. E., *Macromol. Chem. Phys.*, 1994, **195**, 3103.
67. van Streun, K. H., Belt, W. J., Piet, P. and German, A. L., *Euro Polym. J.*, 1991, **27**, 931.
68. Lane, W. H., *Ind. Eng. Chem.*, 1946, **18**, 295.
69. Hough, D. B. and White, L. R., *Adv. Colloid Interface Sci.*, 1980, **14**, 3.
70. Israelachvili, J. N., *Intermolecular and Surface Forces*. Academic, London, 1992.
71. Russell, G. T., Napper, D. H. and Gilbert, R. G., *Macromolecules*, 1988, **21**, 2133.
72. Tobolsky, A. V. and Offenbach, J., *J. Polym. Sci.*, 1955, **16**, 311.
73. Wilke, C. R. and Chang, P., *A.I.Ch.E.J.*, 1955, **1**, 264.
74. Behrman, E. J. and Edwards, J. O., *Rev. Inorg. Chem.*, 1980, **2**, 179.
75. Jobe, D. J. and Reinsborough, V. C., *Can. J. Chem.*, 1984, **62**, 280.
76. Giannetti, E., *A.I.Ch.E.J.*, 1993, **39**, 1210.
77. Ahmed, S. M., El-Aasser, M. S., Micale, F. J., Poehlein, G. W., Vanderhoff, J. W., in *Polymer Colloids II*, ed. Fitch, RM. Plenum, New York, 1980, p. 265.
78. Dunn, A. S. and Chong, L. C. H., *Br. Polym. J.*, 1970, **2**, 49.
79. Scheren, P. A. G. M., Russell, G. T., Sangster, D. F., Gilbert, R. G. and German, A. L., *Macromolecules*, 1995, **28**, 3637.